International Journal of Innovative
Computing, Information and Control
Volume 11, Number 2, April 2015

ICIC International ©2015 ISSN 1349-4198
pp. 627–640

# HIGH DEGREE CUBATURE $H$-INFINITY FILTER FOR A CLASS OF NONLINEAR DISCRETE-TIME SYSTEMS

Sisi Wang[1,2], Guoqing Qi[1] and Lijun Wang[2]

[1]School of Information Science and Technology
Dalian Maritime University
No. 1, Linhai Road, Ganjingzi District, Dalian 116026, P. R. China
mars32lin@sina.com.cn

[2]School of Navigation
Guangdong Ocean University
No. 48, Jiefang Road, Xiashan District, Zhanjiang 524000, P. R. China

Received March 2014; revised August 2014

Abstract. *This paper brings up an improved high degree cubature H-infinity filter for a class of nonlinear discrete-time systems with non-Gaussian and colored system noises. The proposed H-infinity filter is deduced by introducing the fifth-degree spherical-radial rule into a frame of nonlinear point-based H-infinity filters. Stability analysis demonstrates that the high degree cubature H-infinity filter can effectively improve the stability of standard high degree cubature Kalman filter. Furthermore, the improved filter is contrastively tested in two different classic nonlinear problems with three kinds of uncertain system noises. Simulation results show that the proposed filter achieves better performance in filtering accuracy and robustness than other compared nonlinear filters.*
**Keywords:** Kalman filter, Fifth-degree cubature rule, Target tracking, Nonlinear filtering, $H$-infinity

1. **Introduction.** Recently, a high degree cubature Kalman filter (HCKF) is proposed by B. Jia et al., which has superior performance in high-dimension estimation to the traditional nonlinear filters such as cubature Kalman filter (CKF), unscented Kalman filter (UKF), particle filter and Gauss-Hermite quadrature filter. To guarantee approximate suboptimal linear minimum mean square error of system state estimation, the process and measurement noises are assumed to be the independent white noise sequences with zero means in traditional HCKF and other traditional nonlinear filters [1]. However, the assumption may decrease filtering performance in many practical problems with non-Gaussian, time-variant or colored noises [2, 3, 4, 5, 6, 7]. Furthermore, for nonlinear dynamical systems with large uncertainties, for example, long term orbit uncertainty propagation and magnetometer-based space craft altitude estimation, the statistical properties of the system noises are liable to be unknown, which also limits the stability and accuracy performances of traditional HCKF [1].

One of the promising solution is to improve the traditional HCKF to the corresponding nonlinear $H$-infinity filter. Over the past decade, various nonlinear $H$-infinity filters are brought up based on traditional nonlinear filters, such as extended $H$-infinity filter (EHF), unscented $H$-infinity filter (UHF) and cubature $H$-infinity filter (CHF) [8, 9, 10, 11, 12, 13, 14, 15]. Unlike traditional nonlinear filters which need an exact and accurate system model as well as perfect knowledge of noise statistics, nonlinear $H$-infinity filters require no prior statistical knowledge of the noise with finite bounded energies, and minimize the effect

of the worst possible disturbances on the estimation errors. Therefore, the nonlinear $H$-infinity filter has wide application, ranging from maneuvering target tracking, integrated navigation, positioning to information fusion. Moreover, the presented research works indicate that the performance of traditional nonlinear filter is positively correlated with that of the corresponding nonlinear $H$-infinity filter. Accordingly, an improved nonlinear $H$-infinity filter is brought up based on HCKF, which has not been investigated.

The main contributions of this paper is to propose a high-degree cubature $H$-infinity filter (HCHF) for a class of nonlinear discrete-time systems. The improved algorithm aims to achieve higher accuracy than EHF, UHF and CHF, with better stability and robustness than the HCKF. The solution is to generalize a common frame of nonlinear $H$-infinity filters and introduce the fifth degree spherical-radial rule into the frame. So the intractable Gaussian integrals encountered in the nonlinear $H$-infinity filtering can be approximated using a set of deterministically chosen fifth-degree cubature points. In the end, stability analysis and simulation contrast tests are done to verify the effectiveness. The rest of the paper is organized as follows. The problem is formulated in Section 2. In Section 3, the nonlinear point-based $H$-infinity filters are briefly described, and the HCHF is proposed. Section 4 analyzes the stability of the improved filter. Contrast tests of maneuvering target tracking and demodulation of frequency signals are provided in Section 5. Section 6 concludes the paper.

## 2. Problem Statement.

### 2.1. System description.

A considered nonlinear discrete-time system can be given by

$$\begin{aligned} \mathbf{x}_k &= f\left(\mathbf{x}_{k-1}\right) + \mathbf{v}_{k-1} \\ \mathbf{z}_k &= h\left(\mathbf{x}_k\right) + \mathbf{w}_k \\ \mathbf{y}_k &= \mathbf{L}_k \mathbf{x}_k \end{aligned} \tag{1}$$

where $k$ is a discrete time index; $\mathbf{x}_k \in \mathbb{R}^n$ and $\mathbf{z}_k \in \mathbb{R}^m$ are the system state and measurement at discrete time $k$, respectively; $f : \mathbb{R}^n \times \mathbb{R}^l \to \mathbb{R}^n$ and $h : \mathbb{R}^m \times \mathbb{R}^l \to \mathbb{R}^m$ are some known nonlinear functions. $\mathbf{L}_k$ is an arbitrary known matrix which can be linearly combined to the state $\mathbf{x}_k$. Usually, we make $\mathbf{L}_k$ equal to an identity matrix with appropriate dimension to simplify computation. $\{\mathbf{v}_k\}$ and $\{\mathbf{w}_k\}$ are energy bounded $l_2\left[0, +\infty\right)$ process and measurement noise sequences separately which are defined as the following.

$$\sum\nolimits_{k=0}^{\infty} \mathbf{w}_k^T \mathbf{w}_k < \infty, \ \ \sum\nolimits_{k=0}^{\infty} \mathbf{v}_k^T \mathbf{v}_k < \infty$$

where the superscript '$T$' denotes the matrix transpose. The statistical properties of process noise $\mathbf{v}_k$ and measurement noise $\mathbf{w}_k$ are unknown.

The initial state is $\mathbf{x}_0$, and associated covariance is $\mathbf{P}_0$. $\mathbf{x}_0$ is uncorrelated with $\{\mathbf{w}_k\}$ and $\{\mathbf{v}_k\}$. Let $\hat{\mathbf{y}}_k = F_f\left(\mathbf{Z}_k\right)$ denote the estimate of $\mathbf{y}_k$, when the measurements $\mathbf{Z}_k = \{\mathbf{z}_1, \mathbf{z}_2, \cdots, \mathbf{z}_k\}$ are given. The estimation error is defined as below.

$$\mathbf{e}_k = \hat{\mathbf{y}}_k - \mathbf{L}_k \mathbf{x}_k \tag{2}$$

Let $T_k\left(F_f\right)$ denote the transfer operator that maps the unknown disturbances to the estimation errors. And the $H$-infinity norm of the transfer operator $T_k\left(F_f\right)$ is defined as the following.

$$\left\|T_k\left(F_f\right)\right\|_\infty \triangleq \sup_{\mathbf{x}_0, \{\mathbf{v}_m\}, \{\mathbf{w}_m\} \in l_2} \frac{\sum\limits_{m=0}^{k} \left\|\mathbf{e}_m\right\|_2^2}{\left(\left\|\mathbf{x}_0 - \hat{\mathbf{x}}_{0|0}\right\|_{\mathbf{P}_0^{-1}}^2 + \sum\limits_{m=0}^{k} \left\|\mathbf{v}_m\right\|_{\mathbf{Q}_0^{-1}}^2 + \sum\limits_{m=0}^{k} \left\|\mathbf{w}_m\right\|_{\mathbf{R}_0^{-1}}^2\right)} \tag{3}$$

where the process noise $\mathbf{v}_k$, the measurement noise $\mathbf{w}_k$ and the initial state error $\mathbf{x}_0 - \hat{\mathbf{x}}_{0|0}$ are regarded as unknown disturbances to the estimation error $\mathbf{e}_k$, where $\hat{\mathbf{x}}_{0|0}$ is a priori estimate of $\mathbf{x}_0$. The notation $\|\mathbf{A}\|^2_{\sigma^{-1}}$ is defined as the square of the weighted $l_2$ norm of $\mathbf{A}$, that is to say $\|\mathbf{A}\|^2_{\sigma^{-1}} = \mathbf{A}^T\sigma^{-1}\mathbf{A}$. $\mathbf{Q}_0$ and $\mathbf{R}_0$ are the initial covariances of corresponding noise.

2.2. **Problem formulation.** The HCHF strengthens the filtering robustness and accuracy by making the norm of $T_k(F_f)$ satisfy:

$$\|T_k(F_f)\|_\infty < \gamma^2 \tag{4}$$

where $\gamma > 0$ is a given scalar, standing for error attenuation parameter. The main work in the paper includes:

(i) Considering the system (1), generalize a universal frame of point-based nonlinear $H$-infinity filters.

(ii) Using the fifth-degree spherical-radial rule and the frame presented in (i), establish the HCHF algorithm.

(iii) The HCHF is applied to solve two typical nonlinear problems, and contrast tests are done compared to CHF, UHF and HCKF.

## 3. High Degree $H$-infinity Cubature Filter.

3.1. **Point-based nonlinear $H$-infinity filter.** In this section, a frame of point-based nonlinear $H$-infinity filters is briefly generalized. Considering a class of nonlinear discrete-time system described by Equation (1), a suboptimal nonlinear $H$-infinity filter consists of time update and measurement update two steps [9, 10]. The two steps both involve Gaussian integrals calculations to obtain probability density functions (PDFs) and likelihood functions of system state because they are partly derived from Gaussian filter. These types of integrals are generally intractable unless it is approximated by different quadrature rules which lead to different nonlinear $H$-infinity filters, such as, the UHF based on UT transformation, the CHF based on 3rd-degree cubature rule. If any Gaussian integral $\mathrm{I}(f)$ in suboptimal nonlinear $H$-infinity filters is approximated by the following quadrature rule, then the class of suboptimal nonlinear $H$-infinity filters can be called point-based nonlinear $H$-infinity filters.

$$\mathrm{I}(f) = \int_{\mathbb{R}^n} f(\mathbf{x}) N(\mathbf{x}; \mathbf{0}, \mathbf{P})\, d\mathbf{x} \approx \sum_{i=1}^{N_u} W_i f(\mathbf{\Lambda}_i) \tag{5}$$

where $N_u$ is the total number of quadrature points; $\mathbf{\Lambda}_i$ and $W_i$ are the quadrature points and weights, respectively; $f(\cdot)$ is a known nonlinear function, $N(\mathbf{x}; 0, \mathbf{P})$ is a Gaussian density with argument $\mathbf{x}$, zero mean, and covariance $\mathbf{P}$.

The complete solution of them can be summarized as the following.

**Time Update**

Evaluate predicted state $\hat{\mathbf{x}}_{k|k-1}$ and the associated covariance $\mathbf{P}_{k|k-1}$.

$$\begin{aligned} \hat{\mathbf{x}}_{k|k-1} &= \sum_{i=1}^{N_u} W_i f\left(\mathbf{X}_{i,k-1|k-1}\right) \\ \mathbf{P}_{k|k-1} &= \sum_{i=1}^{N_u} W_i \left(\mathbf{X}_{i,k-1|k-1} - \hat{\mathbf{x}}_{k|k-1}\right)\left(\mathbf{X}_{i,k-1|k-1} - \hat{\mathbf{x}}_{k|k-1}\right)^T + \mathbf{Q}_0 \end{aligned} \tag{6}$$

where the propagated point $\mathbf{X}_{i,k-1|k-1}$ is evaluated from the following state equation.

$$\mathbf{X}_{i,k-1|k-1} = \mathbf{S}_{k-1|k-1}\boldsymbol{\varsigma}_i + \hat{\mathbf{x}}_{k-1|k-1} \tag{7}$$

where $\mathbf{P}_{k-1|k-1} = \mathbf{S}_{k-1|k-1}\left(\mathbf{S}_{k-1|k-1}\right)^T$; $\mathbf{S}_{k-1|k-1}$ can be obtained from the cholesky decomposition or the singular value decomposition of error covariance $\mathbf{P}_{k-1|k-1}$ at discrete time $k-1$.

**Measurement Update**

Update state $\hat{\mathbf{x}}_{k|k}$ and the associated error covariance $\mathbf{P}_{k|k}$.

$$\begin{aligned}\hat{\mathbf{x}}_{k|k} &= \hat{\mathbf{x}}_{k|k-1} + \mathbf{P}_{\mathbf{xz},k|k-1}\mathbf{P}^{-1}_{\mathbf{zz},k|k-1}\left(\mathbf{z}_k - \hat{\mathbf{z}}_{k|k-1}\right)\\ \mathbf{P}_{k|k} &= \mathbf{P}_{k|k-1} - \begin{bmatrix}\mathbf{P}_{\mathbf{xz},k|k-1} & \mathbf{P}_{k|k-1}\end{bmatrix}\cdot {\mathbf{R}'}^{-1}_{e,k}\begin{bmatrix}\mathbf{P}^T_{\mathbf{xz},k|k-1}\\ \mathbf{P}^T_{k|k-1}\end{bmatrix}\end{aligned} \tag{8}$$

where

$$\mathbf{R}'_{e,k} = \begin{bmatrix}\mathbf{P}_{\mathbf{zz},k|k-1} & \mathbf{P}^T_{\mathbf{xz},k|k-1}\\ \mathbf{P}_{\mathbf{xz},k|k-1} & \mathbf{P}_{k|k-1} - \gamma^2\mathbf{I}\end{bmatrix}$$

where $\mathbf{I}$ is an identity matrix with appropriate dimension. $\gamma$ is adjusted as following to guarantee the positiveness of $\mathbf{P}_{k|k}$ [9].

$$\gamma_k^2 = \beta\max\left\{\mathrm{eig}\left(\mathbf{P}^{-1}_{k|k-1} + \mathbf{P}^{-1}_{k|k-1}\mathbf{P}_{\mathbf{xz},k|k-1}\mathbf{R}_0^{-1}\left[\mathbf{P}^{-1}_{k|k-1}\mathbf{P}_{\mathbf{xz},k|k-1}\right]^T\right)^{-1}\right\} \tag{9}$$

where $\beta$ is a scalar bigger than one; $\max\left\{\mathrm{eig}\left(\mathbf{A}\right)^{-1}\right\}$ denotes the maximum eigenvalue of the matrix $\mathbf{A}^{-1}$.

Predicted measurement $\hat{\mathbf{z}}_{k|k-1}$ is given by the following equation.

$$\hat{\mathbf{z}}_{k|k-1} = \sum_{i=1}^{N_u} W_i\mathbf{Z}_{i,k|k-1} \tag{10}$$

The covariance and cross-covariance of predicted measurement are given

$$\begin{aligned}\mathbf{P}_{\mathbf{xz},k|k-1} &= \sum_{i=1}^{N_u} W_i\left(\mathbf{X}_{i,k|k-1} - \hat{\mathbf{x}}_{k|k-1}\right)\left(\mathbf{Z}_{i,k|k-1} - \hat{\mathbf{z}}_{k|k-1}\right)^T\\ \mathbf{P}_{\mathbf{zz},k|k-1} &= \sum_{i=1}^{N_u} W_i\left(\mathbf{Z}_{i,k|k-1} - \hat{\mathbf{z}}_{k|k-1}\right)\left(\mathbf{Z}_{i,k|k-1} - \hat{\mathbf{z}}_{k|k-1}\right)^T + \mathbf{R}_0\end{aligned} \tag{11}$$

where the predicted transformed points $\mathbf{X}_{i,k|k-1}$ and measurement propagated points $\mathbf{Z}_{i,k|k-1}$ are defined by Equation (12).

$$\begin{aligned}\mathbf{X}_{i,k|k-1} &= \mathbf{S}_{k|k-1}\boldsymbol{\varsigma}_i + \hat{\mathbf{x}}_{k|k-1}\\ \mathbf{Z}_{i,k|k-1} &= h\left(\mathbf{X}_{i,k|k-1}\right)\end{aligned} \tag{12}$$

and factor $\mathbf{S}_{k|k-1}$ can be obtained from the $\mathbf{P}_{k|k-1}$ with similar decomposition to $\mathbf{S}_{k-1|k-1}$.

The quadrature points $\boldsymbol{\varsigma}_i$ and weights $W_i$ can be obtained through many numerical rules, such as unscented transformation, 3rd-degree cubature rule, and Gauss-Hermite quadrature rule. For example, if the unscented transformation is adapted, $N_u = 2n+1$; the symmetric points $\boldsymbol{\varsigma}_i$ and weights $W_i$ are given by [16]:

$$\begin{cases}\boldsymbol{\varsigma}_i = [0,\ldots,0]^T, & W_i = \kappa/n+\kappa, \quad i = 1\\ \boldsymbol{\varsigma}_i = \sqrt{n+\kappa}\,\mathbf{e}_{i-1}, & W_i = 1/(2(n+\kappa)), \quad 2\le i\le n+1\\ \boldsymbol{\varsigma}_i = -\sqrt{n+\kappa}\,\mathbf{e}_{i-n-1}, & W_i = 1/(2(n+\kappa)), \quad n+2\le i\le 2n+1\end{cases} \tag{13}$$

where $\mathbf{e}_{i-1}$ is the unit vector in $\mathbb{R}^n$ with the $(i-1)^{th}$ element being 1 and $\kappa$ is a scalar with the suggested optimal value of $\kappa = 3-n$. Note that the 3rd-degree cubature rule has the identical form with the unscented transformation if $\kappa = 0$.

**Remark 3.1.** *It should be noted that point-based H-infinity filters have the similar structures to the traditional point-based filters. The only difference between point-based H-infinity filters and traditional ones is the solution to obtain error covariance* $\mathbf{P}_{k|k}$ *as shown in Equation (8). Furthermore, when* $\gamma_k \to \infty$*, the point-based H-infinity filters reduce to the corresponding traditional ones. The parameter* $\gamma_k$ *can be seen as the tuning factor, to make point-based H-infinity filters reach equilibrium between H-infinity performance and approximately minimum variance performance.*

### 3.2. **High degree cubature *H*-infinity filter.**

3.2.1. *High degree cubature rule.* The high-degree cubature rule refers mostly to the 5th-degree cubature rule. Similar to the 3rd-degree cubature rule, it is still approximated efficiently to the Gaussian weighted integral by a set of corresponding 5th-degree cubature points and weights. The Gaussian integer as in Equation (5) is approximated by 5th-degree cubature rule as the following [1].

$$\begin{aligned}\mathrm{I}(f) \approx{}& \frac{2}{n+2} f(0) + \frac{1}{(n+2)^2} \sum_{i=1}^{n(n-1)/2} \left( f\left(\sqrt{n+2}\cdot \mathbf{s}_i^+\right)\right.\\ &\left. + f\left(-\sqrt{n+2}\cdot \mathbf{s}_i^+\right)\right) + \frac{1}{(n+2)^2} \sum_{i=1}^{n(n-1)/2} \left( f\left(\sqrt{n+2}\cdot \mathbf{s}_i^-\right)\right.\\ &\left. + f\left(-\sqrt{n+2}\cdot \mathbf{s}_i^-\right)\right) + \frac{4-n}{2(n+2)^2} \sum_{j=1}^{n} \left( f\left(\sqrt{n+2}\cdot \mathbf{e}_j\right)\right.\\ &\left. + f\left(-\sqrt{n+2}\cdot \mathbf{e}_j\right)\right)\end{aligned} \tag{14}$$

where the point of $\mathbf{s}_i^+$ and $\mathbf{s}_i^-$ are given by

$$\begin{aligned}\left\{\mathbf{s}_i^+\right\} &\triangleq \left\{ \sqrt{\frac{1}{2}} (\mathbf{e}_k + \mathbf{e}_l) : k < l, k, l = 1, 2, \ldots, n \right\}\\ \left\{\mathbf{s}_i^-\right\} &\triangleq \left\{ \sqrt{\frac{1}{2}} (\mathbf{e}_k - \mathbf{e}_l) : k < l, k, l = 1, 2, \ldots, n \right\}\end{aligned} \tag{15}$$

The total number of 5th-degree cubature points $N_u$ is equal to $2n^2 + 1$. According to Equation (14), we have the cubature points and weights of 5th-degree cubature rule as the following.

$$\begin{cases} \boldsymbol{\varsigma}_i = [0, \ldots, 0]^T, \quad W_1 = 2/(n+2), \quad i = 0 \\ \boldsymbol{\varsigma}_i^+ = \sqrt{n+2}\mathbf{s}_i^+, \quad \boldsymbol{\varsigma}_i^- = \sqrt{n+2}\mathbf{s}_i^-, \quad W_i = 1/(n+2)^2, \quad 1 \le i \le n(n-1)/2 \\ \boldsymbol{\varsigma}_i^+ = -\sqrt{n+2}\mathbf{s}_{i-n(n-1)/2-1}^+, \quad \boldsymbol{\varsigma}_i^- = -\sqrt{n+2}\mathbf{s}_{i-n(n-1)/2-1}^-, \quad W_i = 1/(n+2)^2, \\ \qquad\qquad n(n-1)/2 + 1 \le i \le n(n-1) \\ \boldsymbol{\varsigma}_j^e = \sqrt{n+2}\mathbf{e}_j, \quad W_j = (4-n)/\left[2(n+2)^2\right], \quad 1 \le j \le n \\ \boldsymbol{\varsigma}_j^e = -\sqrt{n+2}\mathbf{e}_{j-n-1}, \quad W_j = (4-n)/\left[2(n+2)^2\right], \quad n+1 \le j \le 2n \end{cases} \tag{16}$$

**Remark 3.2.** *Some weights of 5th-degree cubature points maybe negative, and they are less stable than that of 3rd-degree cubature points, just as the UT with* $\kappa = 3 - n$ *is less stable than the 3rd-degree cubature rule, especially for large n. However, the 5th-degree cubature rules behave very differently from the UT with* $\kappa = 3 - n$*. As* $n \to \infty$*, the negative weight in the UT (see Equation (13)) goes to* $-\infty$*, but the negative weight in the*

*5th-degree cubature rule goes to 0 (see Equation (16)). The weights of the cubature rules are therefore much more balanced.*

3.2.2. *High degree cubature H-infinity filter.* In this section, HCHF is proposed by introducing the 5th cubature points and weights into the frame of point-based $H$-infinity filter Equations (6)-(12). The time-update and measurement steps of HCHF are denoted as the following.

The initial state estimates $\hat{\mathbf{x}}_{k-1|k-1}$ and associated covariance $\mathbf{P}_{k-1|k-1}$ are both known quantity.

**Time Update**

(1) In practice, due to errors introduced by arithmetic operations performed on finite word-length digital computers, the error covariance is likely to turn out to be non-positive definite. Therefore, we apply the singular value decomposition to $\mathbf{P}_{k-1|k-1}$ instead of Cholesky decomposition which is limited to positive definite matrix.

$$\mathbf{P}_{k-1|k-1} = \mathbf{U}_{k-1|k-1}\mathbf{S}_{k-1|k-1}\mathbf{V}^T_{k-1|k-1} \tag{17}$$

where $\mathbf{S}_{k-1|k-1}$ is a diagonal matrix, $\mathbf{U}_{k-1|k-1}$ and $\mathbf{V}_{k-1|k-1}$ are both unitary matrices.

(2) Evaluate the cubature points $(i = 1, 2, \cdots, n\,(n-1),\ j = 1, 2, \cdots, 2n)$

$$\begin{aligned}
\mathbf{X}^+_{i,k-1|k-1} &= \mathbf{U}_{k-1|k-1}\sqrt{\mathbf{S}_{k-1|k-1}}\boldsymbol{\varsigma}^+_i + \hat{\mathbf{x}}_{k-1|k-1} \\
\mathbf{X}^-_{i,k-1|k-1} &= \mathbf{U}_{k-1|k-1}\sqrt{\mathbf{S}_{k-1|k-1}}\boldsymbol{\varsigma}^-_i + \hat{\mathbf{x}}_{k-1|k-1} \\
\mathbf{X}_{j,k-1|k-1} &= \mathbf{U}_{k-1|k-1}\sqrt{\mathbf{S}_{k-1|k-1}}\boldsymbol{\varsigma}^e_j + \hat{\mathbf{x}}_{k-1|k-1}
\end{aligned} \tag{18}$$

(3) Estimate the predicted state

$$\begin{aligned}
\hat{\mathbf{x}}_{k|k-1} = &\frac{2}{n+2} f\left(\hat{\mathbf{x}}_{k-1|k-1}\right) + \frac{1}{(n+2)^2}\sum_{i=1}^{n(n-1)}\Big(f\left(\mathbf{X}^+{}_{i,k-1|k-1}\right) \\
&+ f\left(\mathbf{X}^-{}_{i,k-1|k-1}\right)\Big) + \frac{4-n}{2(n+2)^2}\sum_{j=1}^{2n} f\left(\mathbf{X}_{j,k-1|k-1}\right)
\end{aligned} \tag{19}$$

(4) Estimate the predicted error covariance

$$\begin{aligned}
\mathbf{P}_{k|k-1} = &\frac{2}{n+2} f\left(\mathbf{x}_{k-1|k-1}\right) f^T\left(\mathbf{x}_{k-1|k-1}\right) \\
&+ \frac{1}{(n+2)^2}\sum_{i=1}^{n(n-1)}\Big(f\left(\mathbf{X}^+{}_{i,k-1|k-1}\right) f^T\left(\mathbf{X}^+{}_{i,k-1|k-1}\right) \\
&+ f\left(\mathbf{X}^-{}_{i,k-1|k-1}\right) f^T\left(\mathbf{X}^-{}_{i,k-1|k-1}\right)\Big) \\
&+ \frac{4-n}{2(n+2)^2}\sum_{j=1}^{2n} f\left(\mathbf{X}_{j,k-1|k-1}\right) f^T\left(\mathbf{X}_{j,k-1|k-1}\right) \\
&- \hat{\mathbf{x}}_{k|k-1}\hat{\mathbf{x}}^T_{k|k-1} + \mathbf{Q}_0
\end{aligned} \tag{20}$$

**Measurement Update**

(1) Singular value decomposition of predicted error covariance.

$$\mathbf{P}_{k|k-1} = \mathbf{U}_{k|k-1}\mathbf{S}_{k|k-1}\mathbf{V}^T_{k|k-1} \tag{21}$$

where $\mathbf{S}_{k|k-1}$ is a diagonal matrix, $\mathbf{U}_{k|k-1}$ and $\mathbf{V}_{k|k-1}$ are both unitary matrices.

(2) Evaluate the cubature points ($i = 1, 2, \cdots, n(n-1)$, $j = 1, 2, \cdots, 2n$)

$$\begin{aligned}
\mathbf{X}^{+}_{i,k|k-1} &= \mathbf{U}_{k|k-1}\sqrt{\mathbf{S}_{k|k-1}}\boldsymbol{\varsigma}^{+}_{i} + \hat{\mathbf{x}}_{k|k-1} \\
\mathbf{X}^{-}_{i,k|k-1} &= \mathbf{U}_{k|k-1}\sqrt{\mathbf{S}_{k|k-1}}\boldsymbol{\varsigma}^{-}_{i} + \hat{\mathbf{x}}_{k|k-1} \\
\mathbf{X}_{j,k|k-1} &= \mathbf{U}_{k|k-1}\sqrt{\mathbf{S}_{k|k-1}}\boldsymbol{\varsigma}^{e}_{j} + \hat{\mathbf{x}}_{k|k-1}
\end{aligned} \tag{22}$$

(3) Estimate the predicted measurement

$$\begin{aligned}
\hat{\mathbf{z}}_{k|k-1} = &\frac{2}{n+2}h\left(\hat{\mathbf{x}}_{k|k-1}\right) + \frac{1}{(n+2)^2}\sum_{i=1}^{n(n-1)}\left(h\left(\mathbf{X}^{+}{}_{i,k|k-1}\right)\right. \\
&\left. + h\left(\mathbf{X}^{-}{}_{i,k|k-1}\right)\right) + \frac{4-n}{2(n+2)^2}\sum_{j=1}^{2n}h\left(\mathbf{X}_{j,k|k-1}\right)
\end{aligned} \tag{23}$$

(4) Estimate the innovation covariance matrix

$$\begin{aligned}
\mathbf{P}_{\mathbf{zz},k|k-1} = &\frac{2}{n+2}h\left(\hat{\mathbf{x}}_{k|k-1}\right)h^{T}\left(\hat{\mathbf{x}}_{k|k-1}\right) \\
&+ \frac{1}{(n+2)^2}\sum_{i=1}^{n(n-1)}\left(h\left(\mathbf{X}^{+}{}_{i,k|k-1}\right)h^{T}\left(\mathbf{X}^{+}{}_{i,k|k-1}\right)\right. \\
&\left. + h\left(\mathbf{X}^{-}{}_{i,k|k-1}\right)h^{T}\left(\mathbf{X}^{-}{}_{i,k|k-1}\right)\right) + \frac{4-n}{2(n+2)^2}\sum_{j=1}^{2n}h\left(\mathbf{X}_{j,k|k-1}\right)h^{T}\left(\mathbf{X}_{j,k|k-1}\right) \\
&- \hat{\mathbf{z}}_{k|k-1}\hat{\mathbf{z}}^{T}_{k|k-1} + \mathbf{R}_{0}
\end{aligned} \tag{24}$$

(5) Estimate the cross-covariance matrix

$$\begin{aligned}
\mathbf{P}_{\mathbf{xz},k|k-1} = &\frac{2}{n+2}\hat{\mathbf{x}}_{k|k-1}h^{T}\left(\hat{\mathbf{x}}_{k|k-1}\right) + \frac{1}{(n+2)^2}\sum_{i=1}^{n(n-1)}\left(\mathbf{X}^{+}{}_{i,k|k-1}h^{T}\left(\mathbf{X}^{+}{}_{i,k|k-1}\right)\right. \\
&\left. + \mathbf{X}^{-}{}_{i,k|k-1}h^{T}\left(\mathbf{X}^{-}{}_{i,k|k-1}\right)\right) + \frac{4-n}{2(n+2)^2}\sum_{j=1}^{2n}\mathbf{X}_{j,k|k-1}h^{T}\left(\mathbf{X}_{j,k|k-1}\right) \\
&- \hat{\mathbf{x}}_{k|k-1}\hat{\mathbf{z}}^{T}_{k|k-1}
\end{aligned} \tag{25}$$

(6) Evaluate the state $\hat{\mathbf{x}}_{k|k}$ and associate covariance $\mathbf{P}_{k|k}$ using Equations (8) and (9).

4. **Stability Analysis of HCHF.** Since the HCHF originates from linear $H$-infinity filter, we can obtain the approximated equation of predicted error covariance of it as the following [9].

$$\mathbf{P}^{H_\infty}_{k+1|k} \approx \mathbf{F}_{k+1}\mathbf{P}^{H_\infty}_{k|k}\mathbf{F}^{T}_{k+1} + \mathbf{Q}_{0} \tag{26}$$

where $\mathbf{F}_{k+1} = \left.\dfrac{\partial f}{\partial \mathbf{x}}\right|_{\mathbf{x}=\hat{\mathbf{x}}_{k|k}}$. And then, substitute Equation (8) into Equation (26), we can obtain

$$\mathbf{P}^{H_\infty}_{k+1|k} \approx \mathbf{F}_{k+1}\mathbf{P}^{H_\infty}_{k|k-1}\mathbf{F}^{T}_{k+1} + \mathbf{Q}_{0} - \mathbf{F}_{k+1}\begin{bmatrix} \mathbf{P}^{H_\infty}_{\mathbf{xz},k|k-1} & \mathbf{P}^{H_\infty}_{k|k-1} \end{bmatrix}\cdot\mathbf{R}'^{-1}_{e,k}\begin{bmatrix} \left(\mathbf{P}^{H_\infty}_{\mathbf{xz},k|k-1}\right)^{T} \\ \left(\mathbf{P}^{H_\infty}_{k|k-1}\right)^{T} \end{bmatrix}\mathbf{F}^{T}_{k+1} \tag{27}$$

If we assume that the states and associated covariance at time $k-1$ of HCHF and traditional HCKF are equal, indicated as the following.

$$\hat{\mathbf{x}}_{k-1|k-1}^{H_\infty} = \hat{\mathbf{x}}_{k-1|k-1}^{HCKF}, \quad \mathbf{P}_{k-1|k-1}^{H_\infty} = \mathbf{P}_{k-1|k-1}^{HCKF} \tag{28}$$

that is to say

$$\mathbf{P}_{k|k-1}^{H_\infty} = \mathbf{P}_{k|k-1}^{HCKF}, \quad \mathbf{P}_{\mathbf{xz},k|k-1}^{H_\infty} = \mathbf{P}_{\mathbf{xz},k|k-1}^{HCKF}, \quad \mathbf{K}_k^{H_\infty} = \mathbf{K}_k^{HCKF} \tag{29}$$

so, we have

$$\mathbf{P}_{k|k}^{HCKF} = \mathbf{P}_{k|k-1}^{H_\infty} - \mathbf{K}_k^{H_\infty} \left(\mathbf{P}_{\mathbf{xz},k|k-1}^{H_\infty}\right)^T \tag{30}$$

Based on the matrix inversion lemma in [17, 18], and substitute Equation (30) into Equation (8). The $\mathbf{R}_{e,k}^{-1}$ is shown as the following.

$$\mathbf{R}_{e,k}^{-1} = \begin{bmatrix} \mathbf{I} & -\left(\mathbf{K}_k^{H_\infty}\right)^T \\ 0 & \mathbf{I} \end{bmatrix} \begin{bmatrix} \left(\mathbf{P}_{\mathbf{zz},k|k-1}^{H_\infty}\right)^{-1} & 0 \\ 0 & \left(\mathbf{P}_{k|k}^{HCKF} - \gamma_k^2 \mathbf{I}\right)^{-1} \end{bmatrix} \begin{bmatrix} \mathbf{I} & 0 \\ -\mathbf{K}_k^{H_\infty} & \mathbf{I} \end{bmatrix} \tag{31}$$

where $\mathbf{K}_k^{H_\infty}$ is the filtering gain of HCHF at discrete time $k$.

Substitute Equation (31) into Equation (27), we can derive the predicted error covariance of HCHF as follows.

$$\begin{aligned} \mathbf{P}_{k+1|k}^{H_\infty} \approx \mathbf{F}_{k+1} &\left[\mathbf{P}_{k|k-1}^{H_\infty} - \mathbf{K}_k^{H_\infty} \left(\mathbf{P}_{\mathbf{xz},k|k-1}^{H_\infty}\right)^T\right] \mathbf{F}_{k+1}^T + \mathbf{Q}_0 \\ &- \mathbf{F}_{k+1} \mathbf{P}_{k|k}^{HCKF} \left[\mathbf{P}_{k|k}^{HCKF} - \gamma_k^2 \mathbf{I}\right]^{-1} \mathbf{P}_{k|k}^{HCKF} \mathbf{F}_{k+1}^T \end{aligned} \tag{32}$$

Substitute Equation (26)and Equation (30) into Equation (32), we get

$$\mathbf{P}_{k+1|k}^{H_\infty} \approx \mathbf{P}_{k+1|k}^{HCKF} + \Delta\mathbf{Q}_{k-1}^{H_\infty} \tag{33}$$

where

$$\Delta\mathbf{Q}_{k-1}^{H_\infty} = -\mathbf{F}_{k+1} \mathbf{P}_{k|k}^{HCKF} \left[\mathbf{P}_{k|k}^{HCKF} - \gamma_k^2 \mathbf{I}\right]^{-1} \mathbf{P}_{k|k}^{HCKF} \mathbf{F}_{k+1}^T \tag{34}$$

let $\mathbf{P}_{k|k}^{HCKF}$ be the eigenvalue decomposition

$$\mathbf{P}_{k|k}^{HCKF} = \mathbf{L} \begin{pmatrix} \vartheta_1 & 0 & \cdots & 0 \\ 0 & \ddots & \ddots & \vdots \\ \vdots & \ddots & \ddots & 0 \\ 0 & \cdots & 0 & \vartheta_n \end{pmatrix} \mathbf{L}^{-1} \tag{35}$$

where $\{\vartheta_k\}$, $k = 1, \ldots, n$ are the eigenvalues of $\mathbf{P}_{k|k}$ and $\mathbf{L}$ is guaranteed as an orthogonal matrix. Thus, $\Delta\mathbf{Q}_{k-1}^{H_\infty}$ can be expressed as follows:

$$\Delta\mathbf{Q}_{k-1}^{H_\infty} = \mathbf{F}_{k+1}\mathbf{L} \begin{pmatrix} -\frac{\vartheta_l^2}{\vartheta_l - \gamma_k^2} & 0 & \cdots & 0 \\ 0 & \ddots & \ddots & \vdots \\ \vdots & \ddots & \ddots & 0 \\ 0 & \cdots & 0 & -\frac{\vartheta_n^2}{\vartheta_n - \gamma_k^2} \end{pmatrix} \left(\mathbf{F}_{k+1}\mathbf{L}\right)^T \tag{36}$$

where $\left\{-\frac{\vartheta_l^2}{\vartheta_l - \gamma_k^2}\right\}$, $l = 1, \ldots, n$ are the eigenvalues of $\Delta\mathbf{Q}_{k-1}^{H_\infty}$. When $\gamma_k$ tends to be positive-infinity, $\Delta\mathbf{Q}_{k-1}^{H_\infty}$ tends to be a zero matrix and the HCHF reduces to a traditional HCKF, if $\gamma_k$ satisfies $\gamma_k^2 > \vartheta_l$, $l = 1, \ldots, n$, then $\Delta\mathbf{Q}_{k-1}^{H_\infty}$ is a positive-definite matrix. Moreover, Equation (8) shows that $\gamma_k$ is greater than all the eigenvalues of $\mathbf{P}_{k|k}$ during the whole filtering procedure. Thus, $\Delta\mathbf{Q}_{k-1}^{H_\infty}$ maintains to be a positive-definite matrix.

It is demonstrated that an extra additive positive-definite matrix in predicted covariance of nonlinear filter can make the filter easier to coverge [19]. Hence, with the help of the $\Delta\mathbf{Q}_{k-1}^{H_\infty}$, HCHF can improve the stability of traditional HCKF. The examples in the next sections further confirm the result.

5. **Simulations Tests.** One of the HCHF goals is to erase the uncertainty of the system noises as much as possible. So the proposed HCHF is applied to two nonlinear problems with three different types uncertain noises setting and compared against the UHF, the CHF and HCKF to demonstrate its performance in this section.

5.1. **Simulations configuration.**

**Example 1**

We consider a communications task of the demodulation of frequency or phase-modulated signals in additive Gaussian white noise, with the modulating signal assumed Gaussian. The frequency modulated signal model which had been discussed using the EHF and UHF [8, 9] can be described by

$$\begin{aligned} \mathbf{x}_k &\triangleq \begin{pmatrix} \omega_k \\ \varphi_k \end{pmatrix} = \begin{pmatrix} \eta\omega_{k-1} + v_{k-1}^1 + \sigma_{k-1}^1 \\ \arctan(\rho\varphi_{k-1} + \omega_{k-1}) + v_{k-1}^2 + \sigma_{k-1}^2 \end{pmatrix} \\ \mathbf{z}_k &\triangleq \begin{pmatrix} z_k^1 \\ z_k^2 \end{pmatrix} = \begin{pmatrix} \cos\varphi_k + w_k^1 \\ \sin\varphi_k + w_k^2 \end{pmatrix} \end{aligned} \tag{37}$$

where $\omega_k$ and $\varphi_k$ are the frequency and phase messages of modulating signal, respectively. $\mathbf{x}_k \triangleq \begin{bmatrix} \omega_k & \varphi_k \end{bmatrix}^T$ and $\mathbf{z}_k \triangleq \begin{bmatrix} z_k^1 & z_k^2 \end{bmatrix}^T$ are the state and measurement vector, respectively. The process and measurement noise $\mathbf{v}_k = \begin{bmatrix} v_k^1 & v_k^2 \end{bmatrix}^T$ and $\mathbf{w}_k = \begin{bmatrix} w_k^1 & w_k^2 \end{bmatrix}^T$ are white Gaussian noises with covariance matrices $\mathbf{Q} = \mathrm{diag}\{3 \quad 30\}$ and $\mathbf{R} = \mathrm{diag}\{1 \quad 1\}$, respectively. $\boldsymbol{\sigma}_k = \begin{bmatrix} \sigma_k^1 & \sigma_k^2 \end{bmatrix}^T$ is assumed to be an extra addictive noise with uniform distribution within $[0, 0.5]$. We take the same values for parameters as in [8, 9], i.e., $\eta = 0.9$, $\rho = 0.99$ and the scalar $\beta$ is chosen to be 4 in (9). The objective is to estimate the frequency message $\omega_k$ from the noise-corrupted measurements $\mathbf{z}_k$.

From the noise settings in the state equation, it can be seen that the actual process noise is uncertain. So, it is difficult to accurately characterize the process noise only by the covariance $\mathbf{Q}$. The initial estimate of state is generated randomly from the normal distribution, which is denoted using $\hat{\mathbf{x}}_{0|0} \sim N\left(\mathbf{x}_0, \mathbf{P}_{0|0}\right)$ with $\mathbf{x}_0$ being the true initial value $\mathbf{x}_0 = \begin{bmatrix} 2000 & 0 \end{bmatrix}^T$ and $\mathbf{P}_{0|0}$ being the initial covariance $\mathbf{P}_{0|0} = \mathrm{diag}(\begin{bmatrix} 200 & 10 \end{bmatrix})$.

**Example 2**

A classic maneuvering target tracking application is considered, which executes maneuvering turn in a horizontal plane at an unknown turn rate [1, 2]. The kinematic of the turning motion can be modeled by the following nonlinear state equation.

$$\mathbf{x}_k = \begin{bmatrix} 1 & \dfrac{\sin\Omega_k\Delta t}{\Omega} & 0 & -\left(\dfrac{1-\cos\Omega_k\Delta t}{\Omega}\right) & 0 \\ 0 & \cos\Omega_k\Delta t & 0 & -\sin\Omega_k\Delta t & 0 \\ 0 & \dfrac{1-\cos\Omega_k\Delta t}{\Omega} & 1 & \dfrac{\sin\Omega_k\Delta t}{\Omega} & 0 \\ 0 & \sin\Omega_k\Delta t & 0 & \cos\Omega_k\Delta t & 0 \\ 0 & 0 & 0 & 0 & 1 \end{bmatrix} \mathbf{x}_{k-1} + \mathbf{v}_k \tag{38}$$

where the target state $\mathbf{x}_k = \begin{bmatrix} x_k & \dot{x}_k & y_k & \dot{y}_k & \Omega_k \end{bmatrix}^T$; $x_k$ and $y_k$ denote the positions, and $\dot{x}_k$ and $\dot{y}_k$ denote velocities in $x$ and $y$ directions, respectively; $\Omega_k$ is the unknown turn rate at time $k$; $\Delta t$ is the time interval between two consecutive measurement; the process

noise $\mathbf{v}_k$ is Gaussian white noise consequences with zero mean, and the covariance $\mathbf{Q}_{k-1}$ satisfies:

$$\mathbf{Q}_{k-1} = diag\left[\begin{array}{ccc} q_1\mathbf{M} & q_1\mathbf{M} & \Delta t \end{array}\right] \tag{39}$$

where

$$\mathbf{M} = \left[\begin{array}{cc} (\Delta t)^3/3 & (\Delta t)^2/2 \\ (\Delta t)^2/2 & \Delta t \end{array}\right]$$

The scalar parameter $q_1$ is related to process noise intensity. A radar is fixed at the origin of the plane and equipped to measure the range $r_k$ and bearing $\theta_k$. Hence, the measurement equation is given by

$$\left(\begin{array}{c} r_k \\ \theta_k \end{array}\right) = \left[\begin{array}{c} \sqrt{x_k^2 + y_k^2} \\ \tan^{-1}\left(\dfrac{y_k}{x_k}\right) \end{array}\right] + \mathbf{w}_k \tag{40}$$

where $\Delta t = 1\text{s}$, $q_1 = 1\text{m}^2\text{s}^{-3}$, the statistical properties of measurement noise $\mathbf{w}_k$ are uncertain, the initial state $\mathbf{x}_0$ and associate covariance $\mathbf{P}_{0|0}$ are given by

$$\begin{aligned} \mathbf{x}_0 &= \left[\begin{array}{ccccc} 1000\text{m} & 300\text{ms}^{-1} & 1000\text{m} & 0\text{ms}^{-1} & -3^\circ\text{s}^{-1} \end{array}\right]^T \\ \mathbf{P}_{0|0} &= \text{diag}\left[\begin{array}{ccccc} 100\text{m}^2 & 10\text{m}^2\text{s}^{-2} & 100\text{m}^2 & 10\text{m}^2\text{s}^{-2} & 100\text{mrad}^2\text{s}^{-2} \end{array}\right] \end{aligned}$$

The initial state estimate $\hat{\mathbf{x}}_{0|0} \sim N\left(\mathbf{x}_0, \mathbf{P}_{0|0}\right)$. In accordance with Equation (38) and the parameters defined above, Figure 1 shows the true trajectory of target during 100 sample times.

For a fair comparison, we make 150 independent Monte Carlo runs. The total number of scans per run is 100. All the filters are initialized with the same condition in each run. To compare the various nonlinear $H$-infinity filter performance, the metrics we introduced is the root mean square error (RMSE). For example, the RMSE in position at time $k$ is defined as

$$\text{RMSE}_{pos,k} = \sqrt{\frac{1}{N}\sum_{n=1}^{N}\left(x_k - \hat{x}_k^n\right)^2 + \left(y_k - \hat{y}_k^n\right)^2}$$

where $(x_k, y_k)$ is the true position at discrete time $k$ and $(\hat{x}_k^n, \hat{y}_k^n)$ is estimated position at discrete time $k$ of the $n^{th}$ Monte Carlo run. Similarly to the RMSE in position, we may also write formulas of the RMSE in frequency message $\omega_k$.

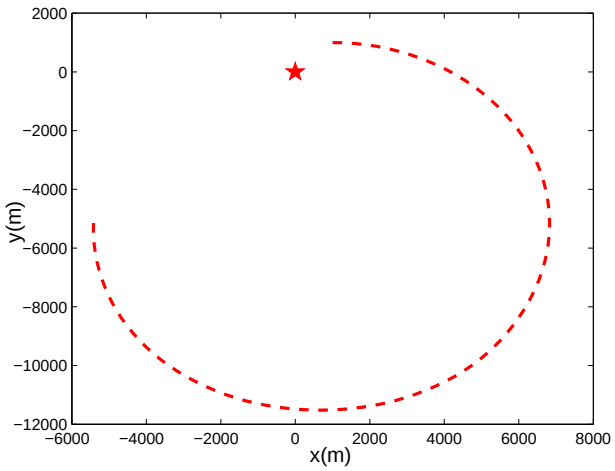


FIGURE 1. True trajectory of target (★-radar location)

5.2. **Simulations results.**

**Example 1**

The RMSEs of frequency message $\omega_k$ are shown in Figure 2. It is observed that at filtering initial stage (the first 30 sampling step or so), the RMSEs of four compared filter are very close. As the filtering goes on, the estimation errors are accumulative. So the RMSEs of UHF and CHF significantly increase, but the RMSEs of HCKF and HCHF are still kept in a narrow, relatively low range, which is far below that of UHF and CHF at same time. To further compare the performances of four filters, all the RMSE mean values are indicated in Table 1. From Table 1, it can be seen that the RMSE mean values of HCHF is smaller than that of HCKF, and the RMSE means of HCKF, CHF and UHF increase in turn.

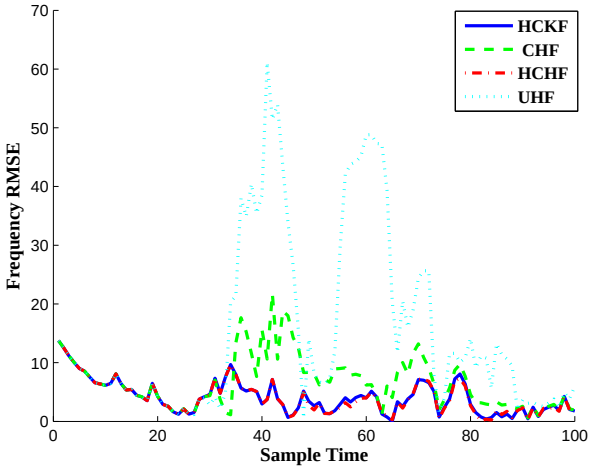


FIGURE 2. RMSEs in frequency message for Example 1

TABLE 1. RMSE means in frequency message for Example 1

| Item \ Algorithms | HCKF | CHF | HCHF | UHF |
|---|---|---|---|---|
| RMSE Means in frequency message | 4.1236 | 6.6675 | 4.0397 | 15.4476 |

**Example 2**

In Example 2, to test the robustness of the HCHF, we make the measurement noise to be non-Gaussian and colored noise, respectively. In view of the importance of target position in radar maneuvering target tracking, the objective of Example 2 is to estimate the target position from the noise-corrupted measurements $r_k$ and $\theta_k$.

**Scenario 1**.

The non-Gaussian measurement noise $\mathbf{w}_k \sim 0.5\mathrm{N}(\mathbf{0}, \mathbf{R}_1) + 0.5\mathrm{N}(\mathbf{0}, \mathbf{R}_2)$, where

$$\mathbf{R}_1 = \begin{bmatrix} 1000\mathrm{m}^2 & 150\mathrm{mmrad} \\ 150\mathrm{mmrad} & 100\mathrm{mrad}^2 \end{bmatrix}$$

$$\mathbf{R}_2 = \begin{bmatrix} 50\mathrm{m}^2 & 100\mathrm{mmrad} \\ 100\mathrm{mmrad} & 1000\mathrm{mrad}^2 \end{bmatrix}$$

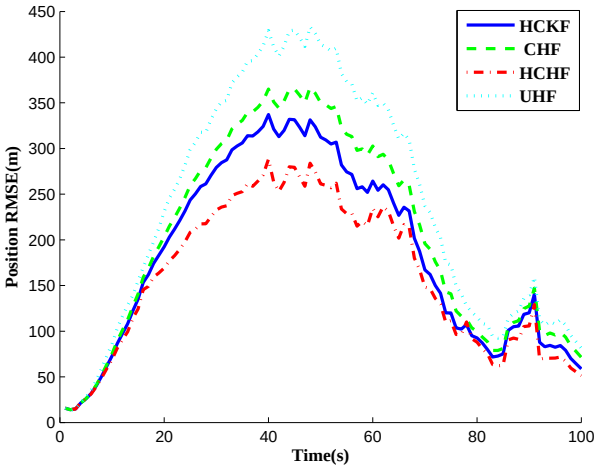


FIGURE 3. RMSEs in position for scenario l

TABLE 2. RMSE means in position for scenario 1

| Item \ Algorithms | HCKF | CHF | HCHF | UHF |
|---|---|---|---|---|
| RMSE Means in Position (m) | 185.0919 | 204.0774 | 160.0430 | 237.6226 |

the HCKF uses an equivalent measurement noise covariance of the above Gaussian mixture model. A similar setup has been used to test the robustness of the 3rd degree CKF and the HCKF [1, 2]. The scalar $\beta$ is set to 25. The RMSEs in position for scenario 1 and the corresponding RMSE means are shown in Figure 3 and Table 2.

As indicated in Figure 3 and Table 2, the HCHF achieves better position tracking performance than other compared filters with position error reductions of 14% to 32% in RMSE mean values. Furthermore, except HCHF, the RMSE in target position of HCKF is much smaller than that of CHF and UHF with position error reductions of 9% and 16% in RMSE mean values. So the RMSEs of four compared filters decline in orders of UHF, CHF, HCKF and HCHF.

**Scenario 2**.

The colored measurement noise $\mathbf{w}_k = \phi_{k,k-1}\mathbf{w}_{k-1} + \boldsymbol{\xi}_{k-1}$, where $\boldsymbol{\xi}_{k-1}$ is a Gaussian white noise consequences with means zero, and the covariance satisfies:

$$\mathbf{R} = \text{diag}\left[\begin{array}{cc} \sigma_r^2 & \sigma_\theta^2 \end{array}\right]$$

where $\sigma_r = 40$m, $\sigma_\theta = 100$mrad. The correlated coefficient $\phi_{k,k-1}$ is chosen to be 0.7.

The HCKF also uses an equivalent measurement noise covariance of above colored noise. The scalar $\beta$ is set to 14. The RMSEs in position for scenario 2 and the corresponding RMSE means are shown in Figure 4 and Table 3.

As shown in Figure 4 and Table 3, the HCHF still performs better than other compared filters in colored measurement noise environment. In terms of RMSE mean values in position, the position tracking precision has been improved by error reductions of 8% to 13%.

Therefore, in Examples 1 and 2, the HCHF generates superior performance to other compared $H$-infinity filters. This is expected due to the fact that the HCHF is carried out based on the 5th-degree spherical-radial rule which provides more accurate performance

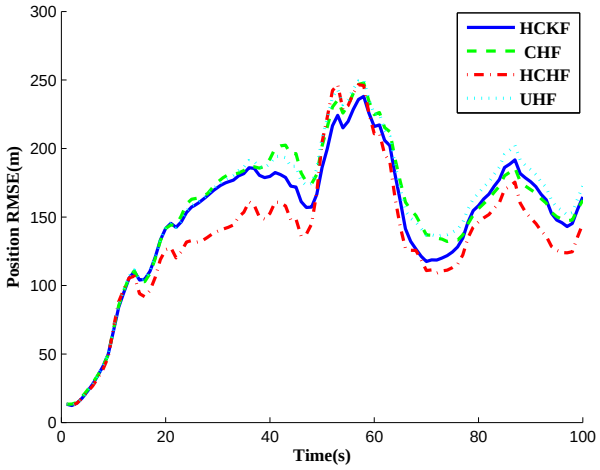


FIGURE 4. RMSEs in position for scenario 2

TABLE 3. RMSE means in position for the various filters for scenario 2

| Item \ Algorithms | HCKF | CHF | HCHF | UHF |
|---|---|---|---|---|
| RMSE Means in Position (m) | 149.8648 | 155.5755 | 137.0812 | 158.0992 |

than other numerical integration rules. Since the HCHF performs better than HCKF, it is illustrated that the HCHF can further improve the robustness of HCKF when the process noise or measurement noise bias from Gaussian distribution. Moreover, it is noted that HCKF performs better than other $H$-infinity filters because it is more robust against model errors and noise uncertainties than other compared traditional nonlinear $H$-infinity filters.

5.3. **Numerical computation cost.** To assess the computational requirements of the proposed method, we compute the averaged CPU time in MATLAB 2009b on a 1.60GHz CPU Celeron-based computer operating under Windows XP System. For Example 1, the HCHF and HCKF require 0.363s and 0.157s, respectively; while the CHF and UHF only need 0.11s and 0.13s. For scenario 1, the HCHF and HCKF require 0.50s and 0.456s, respectively; while the CHF and UHF only need 0.126s and 0.146s. For scenario 2, the HCHF and HCKF require 0.490s and 0.439s, compared with only 0.120s and 0.146s needed by the CHF and UHF. It is obvious that the HCHF has a slightly higher computational cost than the HCKF due to the computational complexity of the updated covariance $\mathbf{P}_{k|k}$ and the extra computation of the tuning parameter $\gamma_k$ in Equation (8). Furthermore, for using the 5th cubature rule, the HCHF computes more slowly than other compared nonlinear $H$-infinity filters.

6. **Conclusion.** In this paper, an improved nonlinear $H$-infinity filtering algorithm is developed by introducing the 5th cubature rule into the frame of nonlinear point-based $H$-infinity filter structure. And then, it is proved that the HCHF can improve the stability of the traditional HCKF. Moreover, simulation results show that the proposed filter is robust to the uncertain system noises and can yield more accurate results than HCKF and other compared nonlinear $H$-infinity algorithms with additional computation cost.

**Acknowledgment.** This work is supported by the National 863 Program (2011AA1102 01).

## REFERENCES

[1] B. Jia, M. Xin and Y. Cheng, High-degree cubature Kalman filter, *Automatica*, vol.49, no.2, pp.510-518, 2013.

[2] I. Arasaratnam and S. Haykin, Cubature Kalman filters, *IEEE Trans. Automatic Control*, vol.54, no.6, pp.1254-1269, 2009.

[3] Q. B. Ge, W. B. Li and C. L. Wen, SCKF-STF-CN: A universal nonlinear filter for maneuver target tracking, *Journal of Zhejiang University Science C*, vol.12, no.8, pp.678-686, 2012.

[4] S. S. Wang and L. J. Wang, Maneuvering target tracking based on adaptive square root cubature Kalman filter algorithm, *Proc. of the 2012 International Conference on Information Technology and Software Engineering*, pp.901-908, 2013.

[5] F. Sun and L. J. Tang, INS/GPS integrated navigation filter algorithm based on cubature Kalman filter, *Control and Decision*, vol.27, no.7, pp.1032-1036, 2012.

[6] W. Li and Y. Jia, Location of mobile station with maneuvers using an IMM-based cubature Kalman filter, *IEEE Trans. Industrial Electronics*, vol.59, no.11, pp.4338-4348, 2012.

[7] B. Chandra, D. W. Gu and I. Postlethwaite, Square root cubature information filter, *IEEE Sensors Journal*, vol.13, no.2, pp.750-758, 2013.

[8] G. A. Einicke and L. B. White, Robust extended Kalman filtering, *IEEE Trans. Signal Processing*, vol.47, no.9, pp.2596-2599, 1999.

[9] W. Li and Y. Jia, $H$-infinity filtering for a class of nonlinear discrete-time systems based on unscented transform, *Signal Processing*, vol.90, no.12, pp.3301-3307, 2010.

[10] B. Chandra, K. Pakkid, D. W. Gu and I. Postlethwaite, Cubature $H_\infty$ information filter, *IEEE European Control Conference*, pp.2639-2644, 2013.

[11] X. Su, P. Shi, L. Wu and M. Basin, Reliable filtering with strict dissipativity for T-S fuzzy time-delay systems, *IEEE Trans. Cybernetics*, 2014.

[12] Y. Yin, P. Shi, F. Lu and K. L. Teo, Fuzzy model-based robust $H$-infinity filtering for a class of nonlinear nonhomogeneous Markov jump systems, *Signal Processing*, vol.93, no.9, pp.2381-2391, 2013.

[13] Z. Wu, P. Shi, H. Su and J. Chu, Asynchronous $l_2$-$l_\infty$ filtering for discrete-time stochastic Markov jump systems with randomly occurred sensor nonlinearities, *Automatica*, vol.1, no.1, pp.180-186, 2014.

[14] Y. Wang, P. Shi, Q. Wang and D. Duan, Exponential $H_\infty$ filtering for singular Markovian jump systems with mixed mode-dependent time-varying delay, *IEEE Trans. Circuits and Systems*, vol.60, no.9, pp.2440-2452, 2013.

[15] P. Shi, X. Luan and F. Liu, $H_\infty$ filtering for discrete-time systems with stochastic incomplete measurement and mixed delays, *IEEE Trans. Industrial Electronics*, vol.59, no.6, pp.2732-2739, 2012.

[16] S. J. Julier, J. K. Uhlmann and H. F. Durrant-Whyte, A new method for the nonlinear transformation of means and covariances in filters and estimators, *IEEE Trans. Automatic Control*, vol.45, no.3, pp.477-482, 2000.

[17] D. Simon, *Optimal State Estimation: Kalman, H Infinity, and Nonlinear Approaches*, John Wiley and Sons, New York, 2006.

[18] H. Poveda, E. Grivef, G. Ferré and N. Christov, Kalman vs $H_\infty$ filter in terms of convergence and accuracy: Application to carrier frequency offset estimation, *Proc. of the 20th IEEE European Signal Processing Conference*, pp.121-125, 2012.

[19] K. Xiong, H. Y. Zhang and C. W. Chan, Performance evaluation of UKF-based nonlinear filtering, *Automatica*, vol.42, no.2, pp.261-270, 2006.